

See discussions, stats, and author profiles for this publication at: <https://www.researchgate.net/publication/231677833>

The Molecular Sieving Mechanism in Carbon Molecular Sieves: A Molecular Dynamics and Critical Path Analysis†

ARTICLE *in* LANGMUIR · MARCH 1997

Impact Factor: 4.46 · DOI: 10.1021/la9510644

CITATIONS

48

READS

10

4 AUTHORS, INCLUDING:



S. P. Friedman

Agricultural Research Organization ARO

70 PUBLICATIONS 1,985 CITATIONS

SEE PROFILE



James M D Macelroy

University College Dublin

116 PUBLICATIONS 1,680 CITATIONS

SEE PROFILE

The Molecular Sieving Mechanism in Carbon Molecular Sieves: A Molecular Dynamics and Critical Path Analysis[†]

N. A. Seaton,^{*,‡} S. P. Friedman,[‡] J. M. D. MacElroy,[§] and B. J. Murphy[§]

Department of Chemical Engineering, University of Cambridge, Pembroke Street, Cambridge CB2 3RA, U.K. and Department of Chemical Engineering, University College Dublin, Belfield, Dublin 4, Ireland

Received November 22, 1995. In Final Form: July 11, 1996[®]

We have investigated the molecular sieving mechanism in carbon molecular sieves (CMSs), by a combination of molecular dynamics simulations and pore network theory, using the separation of air into oxygen and nitrogen as a prototype. Molecular dynamics simulations of diffusion in individual pores show that the diffusion coefficients for oxygen and nitrogen are strong functions of pore width and that the degree of kinetic separation (expressed as the ratio of the species diffusion coefficients) observed experimentally can be reproduced at the level of individual pores. A critical path analysis of diffusion in the pore network of the CMS shows that this degree of kinetic separation can also be obtained with pore networks having a range of pore sizes, even where the width of the pore size distribution is large.

1. Introduction

Carbon molecular sieves (CMSs) are widely used in adsorptive separations. The separation mechanism in CMS-based processes is kinetic in nature. In the case of air separation, for example, there is little difference in the equilibrium adsorption of the two principal components—oxygen and nitrogen—and the separation is due to the difference in the diffusion rates of these species through the pore network. Oxygen diffuses more rapidly than nitrogen; diffusion coefficient ratios between roughly 3 and 30 have been reported.^{1–7}

To some extent, this difference in the diffusion rates is easily understood. Lennard-Jones parameters for the atomic collision diameters are 0.294 nm for oxygen and 0.330 nm for nitrogen,⁸ giving a difference in size of about 10%. These species have similar diffusion coefficients in the bulk, but one would expect their diffusion coefficients to differ in pores that are close to their molecular dimensions. Because of its smaller size, oxygen would be expected to move more rapidly than nitrogen in a small pore. In an ideal limiting case, a constriction of the right size would act as an almost impenetrable barrier to nitrogen but still allow the passage of oxygen.

This type of sieving mechanism is familiar from the study of zeolites, which have a crystalline structure. The sieving mechanism in a CMS, which is only locally crystalline and therefore contains pores of a range of sizes, is more complex. For a microporous carbon to function

as a molecular sieve, it is clear that most of the diffusing molecules must, at some point in their journey to the interior of the adsorbent, encounter constrictions of the right size to exert a sieving effect. For a system of pores in a series, the smallest pore is the dominant resistance to diffusion so that, provided this pore is of the appropriate size, molecular sieving results. The pore network of a real CMS, in contrast, is highly interconnected forming a series–parallel arrangement of resistances to diffusion. Thus, in a real CMS, each diffusing molecule has a very large number of possible routes from the surface of the adsorbent to its interior, each of which is composed of pores of a range of sizes; a “resistances in series” picture is inadequate for this type of structure. The aim of the work reported here was to investigate the sieving mechanism in the CMS pore network and to quantify the relationship between pore structure and sieving performance.

In this paper, we investigate the diffusion of nitrogen and oxygen in individual graphitic pores, and in pore networks, using a combination of molecular dynamics simulation and network theory. The paper is arranged as follows. In section 2, we investigate diffusion in individual pores by carrying out molecular dynamics (MD) simulations of the motion of oxygen and nitrogen molecules in the individual pores. In section 3, we address diffusion in the CMS pore network, in particular, the relationship between pore structure and molecular sieving. The results of our investigation are summarized in section 4.

2. Diffusion in Individual Pores

Pores in activated carbons (such as CMSs) are largely bounded by graphitic planes, and this forms the basis of our single-pore model. In reality, the planes will not be parallel to each other but, for simplicity, we assume that they are. In studies of the equilibrium adsorption in carbons, the graphitic planes are often considered to be structureless. This simplification, while often adequate for equilibrium properties, gives diffusion coefficients that are much higher than those observed experimentally (except where the pore size is very close to the molecular diameter, in which case the diffusion coefficient goes very rapidly to zero with decreasing pore size). A model with some surface structure is therefore required.

* Author to whom correspondence should be addressed. Telephone: (+44) 1223 334786. Fax: (+44) 1223 334796. E-mail: nas3@cheng.cam.ac.uk.

[†] Presented at the Second International Symposium on Effects of Surface Heterogeneity in Adsorption and Catalysis on Solids, held in Poland/Slovakia, September 4–10, 1995.

[‡] University of Cambridge.

[§] University College Dublin.

[®] Abstract published in *Advance ACS Abstracts*, February 15, 1997.

(1) Chihara, K.; Suzuki, M.; Kawazoe, K. *J. Colloid Interface Sci.* **1978**, *64*, 548.

(2) Chihara, K.; Suzuki, M.; Kawazoe, K. *AIChE J.* **1978**, *24*, 237.

(3) Chihara, K.; Suzuki, M. *Carbon* **1978**, *17*, 339.

(4) Ruthven, D. M.; Raghavan, N. S.; Hassan, M. M. *Chem. Eng. Sci.* **1986**, *41*, 1325.

(5) Ruthven, D. M. *Chem. Eng. Sci.* **1992**, *47*, 4305.

(6) Kikkinides, E. S.; Yang, R. T.; Cho, S. H. *Ind. Eng. Chem. Res.* **1993**, *32*, 2714.

(7) Chen, Y. D.; Yang, R. T.; Uawithya, P. *AIChE J.* **1994**, *40*, 577.

(8) Weiner, S. J.; Kollman, P. A.; Nguyen, D. T.; Case, D. A. *J. Comput. Chem.* **1986**, *7*, 230.

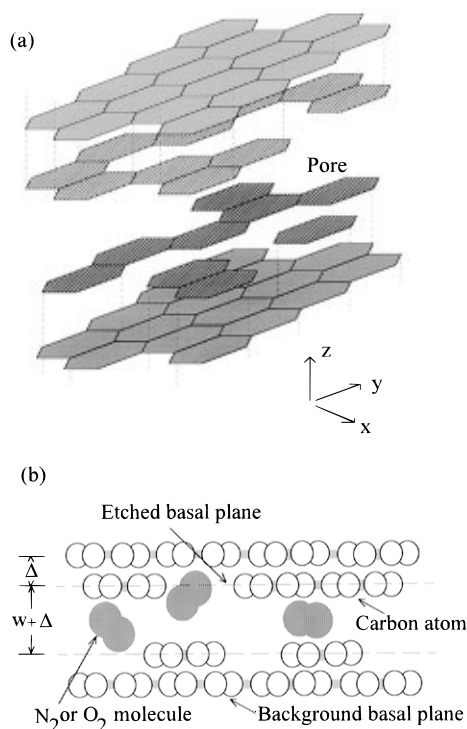


Figure 1. Schematic diagram of an REG pore: (a) a typical etching pattern; (b) a side view.

To simulate the effects of a realistic partially crystalline surface structure, we have developed⁹ the “randomly etched graphite” (REG) model shown in Figure 1. In this model, the innermost graphitic planes are etched (by removal of carbon atoms) so that significant barriers to diffusion exist in the direction parallel to the solid surface. It is worth noting that although the model pore is generated by a process of atom removal, the REG structure could also be considered to be due to carbon deposition, which is one of the steps involved in CMS production. For the purpose of determining the single-pore diffusion coefficients by MD simulations, the REG pore is assumed to be of infinite extent in the x - and y -directions; this is realized by imposing periodic boundary conditions, i.e., by infinitely repeating the fundamental cell in these directions.

The oxygen and nitrogen atoms are modeled as rigid diatomics with bond lengths of 0.1169 nm for oxygen and 0.1097 nm for nitrogen. The interaction between an atom within an oxygen or nitrogen molecule with a carbon atom of the etched graphitic plane in the pore wall is represented by the Lennard-Jones potential

$$\phi_{Ci}(r_{Ci}) = 4\epsilon_{Ci} \left[\left(\frac{\sigma_{Ci}}{r_{Ci}} \right)^{12} - \left(\frac{\sigma_{Ci}}{r_{Ci}} \right)^6 \right] \quad (1)$$

where r_{Ci} is the distance between the two atoms. ϵ_{Ci} and σ_{Ci} are, respectively, the depth of the potential well and the collision diameter for the interaction between the carbon atom and an atom in a gas molecule of species i . ϵ_{Ci} and σ_{Ci} were calculated by applying the Lorentz–Berthelot rules to the pure species potential parameters of Wiener *et al.*⁸ for oxygen and nitrogen and those of Steele¹⁰ for carbon. The parameter values obtained are $\epsilon_{CO}/k_B = 45.98$ K, $\sigma_{CO} = 0.3170$ nm, $\epsilon_{CN}/k_B = 41.12$ K, and

$\sigma_{CN} = 0.3348$ nm. The interaction of the atoms in the gas molecules with the graphite planes further from the center of the pore are represented by the 10-4-3 potential of Steele.¹⁰

MD simulations were carried out to determine the single-pore diffusion coefficients of oxygen and nitrogen in pores of various widths and with various extents of etching. As the separation of oxygen and nitrogen in a CMS primarily reflects the gas–solid, rather than gas–gas, interactions, we restricted ourselves to simulating the motion of single gas molecules (i.e., the low-density or Henry’s law limit). The simulations were carried out in the microcanonical ensemble, in which the total energy of the molecule is constant. The simulation method has been described in detail by MacElroy *et al.*;⁹ here, we restrict ourselves to an outline of the procedure. For each pore size, 200–2000 distinct realizations of an REG pore were created by randomly deleting surface carbon atoms to the desired degree of etching. This large number of realizations is required in order to sample adequately the structural variations observed for a given degree of etching. For each realization, a single molecular trajectory was generated for each of the gas species. The initial position and orientation of the molecule were generated at random, subject to the constraint that the kinetic energy (i.e., the total energy less the potential energy) was positive. The components of the center-of-mass velocity and the angular velocity were assigned at random, consistent with the kinetic energy of the molecule, using the equipartition principle.

The trajectory of the molecule was generated by integrating the equations of motion using the Verlet leapfrog algorithm¹¹ for the translational motion and Fincham’s algorithm¹² for rotational motion. Each simulation consisted of 10^5 time steps, corresponding to a simulated elapsed time of 0 (10^{-9} s). In the simulations, the atom–atom interaction was truncated at $3.5\sigma_{Ci}$ and the potential function was adjusted so that both the potential and its first derivative (i.e., the force) were continuous.⁹ The single-pore diffusion coefficients were calculated using the Green–Kubo equation.¹³

All of the simulations were carried out at values of the total energy corresponding to the mean thermal energy at 300 K. As real molecules diffusing at a given temperature exhibit a Maxwell–Boltzmann distribution of energies, rather than the distribution for an isolated particle in the microcanonical ensemble, the realism of the simulations conducted in the manner described here cannot be taken for granted. For this system, however, MacElroy *et al.*⁹ have demonstrated good agreement between the diffusion coefficients calculated in the microcanonical and canonical (i.e., constant temperature, variable energy) ensemble.

Figure 2 shows the single-pore diffusion coefficients of oxygen and nitrogen, D_O and D_N , respectively, as a function of pore width, w . (w is defined as the distance between the two etched graphitic planes minus the interlayer spacing in graphite, 0.335 nm (see Figure 1b); with this definition, $w = 0$ when the relative positions of the etched planes correspond to adjacent planes in graphite.) In these simulations, the degree of etching was 50%. The diffusion coefficient of nitrogen is immeasurably small, below a pore width of about 0.2 nm, while the diffusion coefficient of oxygen is already substantial for a pore of that width. Diffusion coefficient ratios of the magnitude found experimentally (roughly $R = 3\text{--}30$)^{1–7} are observed in these

(9) MacElroy, J. M. D.; Seaton, N. A.; Friedman, S. P. In *Equilibria and Dynamics of Gas Adsorption on Heterogeneous Solid Surfaces*; Rudzinski, W., Steele, W., Eds.; Elsevier, in press.

(10) Steele, W. A. *The Interaction of Gases with Solid Surfaces*; Pergamon Press: Oxford, 1974.

(11) Hockney, R. W. *Methods Comput. Phys.* **1970**, *9*, 136.

(12) Fincham, D. *CCP5 Q.* **1984**, *12*, 47.

(13) Kubo, R.; Toda, M.; Hashitsume, N. *Statistical Physics II. Nonequilibrium Statistical Mechanics*; Springer-Verlag: Berlin, 1985.

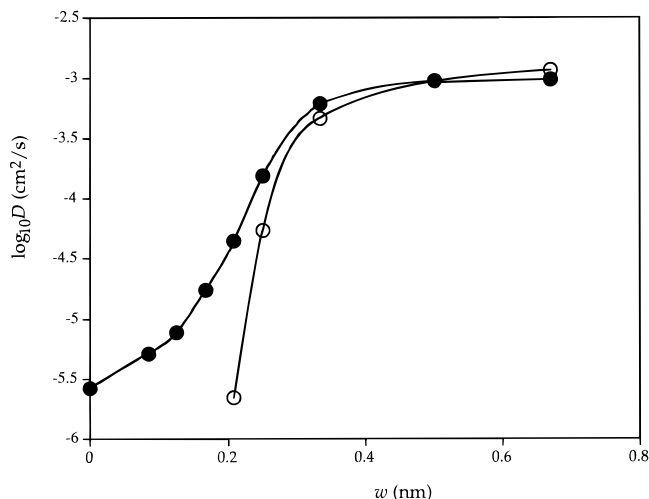


Figure 2. Single-pore diffusion coefficients as a function of pore width for oxygen (solid circles) and nitrogen (open circles). The degree of etching is 50%. The curves are to guide the eye.

simulation results: $R = 20.2$ for $w = 0.209$ nm and $R = 2.80$ for $w = 0.251$ nm.

The influence of the extent of etching is illustrated in parts a and b of Figure 3 for single REG pores of $w = 0.209$ nm and 0.251 nm, respectively. In both of the cases, extents of etching less than about 60% (or equivalently carbon depositions greater than 40%) are required to obtain O_2/N_2 selectivity ratios of 3 or greater. On the other hand, at sufficiently low extents of etching, the nitrogen diffusion coefficient rapidly approaches 0 with the result that the experimentally reported selectivity ratios of 3 to 30 are predicted for a comparatively narrow range of etchings (or depositions). It is of interest to note that this sensitivity to small changes in carbon deposition is known to be a primary feature in the production of commercially viable carbon molecular sieves.

One trend in the results shown in Figure 3b which requires comment is the behavior of the oxygen diffusion coefficient as a function of the extent of etching. For the slit width $w = 0.251$ nm, the increase in the diffusivity as the extent of etching is reduced below 50% is due to the partial confinement of the oxygen molecules at or near the pore center line within the space between the two etched planes. The unetched surfaces of the graphitic planes are essentially smooth, and the diffusive motion is very fast for particles confined within this space. This effect is enhanced at low extents of etching due to the extended range over which the molecules may diffuse before being trapped within the holes in the etched layers. For this slit width, the nitrogen molecule has only very limited access to the volume between the etched planes, so its diffusive behavior is primarily determined by the topology of the holes in the surface planes. (This is simply a reflection of the relative molecular size; for a sufficiently large pore, we would expect nitrogen to show behavior similar to that of oxygen at this pore width.) For the smaller slit width, shown in Figure 3a, both the oxygen and nitrogen molecules are largely confined to these holes.

For the degrees of etching that give a kinetic selectivity in the range observed experimentally, the absolute values of the diffusion coefficients are significantly larger than the single-pore diffusion coefficients deduced from the experimental data. MacElroy *et al.*⁹ have suggested that this may be related to the uncertainty in the appropriate value of the characteristic length used in deducing the diffusion coefficients from the diffusion time constants measured experimentally. A detailed comparison between the predictions of our model and the experimental data

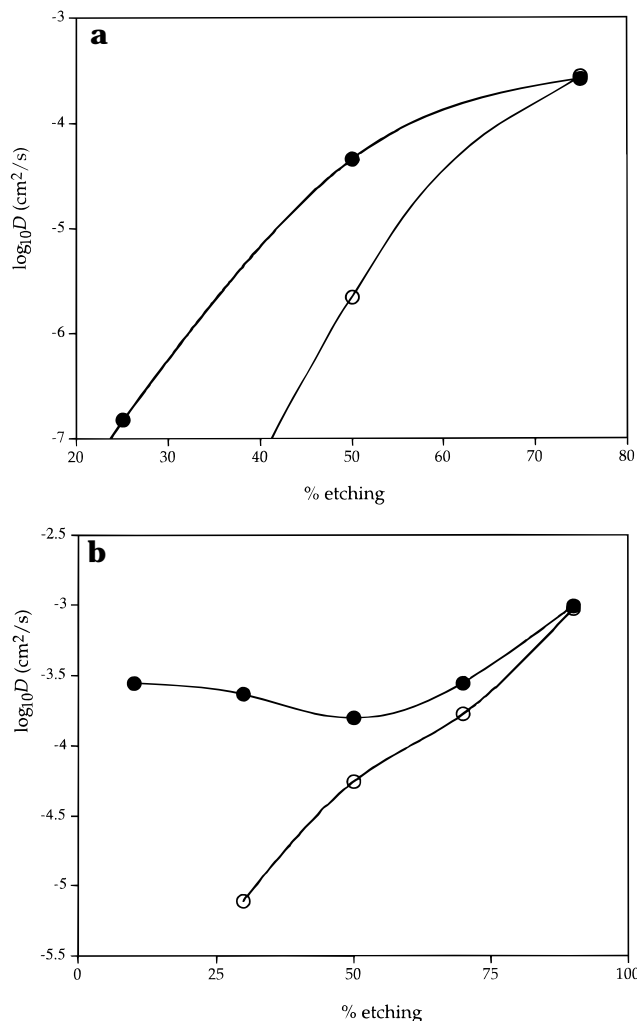


Figure 3. Single-pore diffusion coefficients as a function of the degree of etching for oxygen (solid circles) and nitrogen (open circles). The pore widths are (a) 0.209 nm and (b) 0.251 nm. The curves are to guide the eye. In Figure 3a, the simulated diffusion coefficient for nitrogen is barely measurable (2×10^{-6} cm²/s) at 50% etching; the diffusion coefficients of both of the species are 0 below 25% etching.

for the diffusion coefficients, activation energies, and isosteric heats of adsorption is given by MacElroy *et al.*⁹

3. Molecular Sieving in Pore Networks—Critical Path Analysis

Having demonstrated that the REG model of an individual pore generates diffusion coefficient ratios in the range observed experimentally, we go on to consider diffusion in the pore network of the CMS. Each pore in the network is represented by the REG model with the pore width assigned according to an imposed pore size distribution (PSD) and a mean coordination number, Z , defined to be the mean number of pores meeting at a node in the network. The nodes are considered to be sufficiently large such that they offer no resistance to diffusion. A diffusing molecule thus experiences a succession of openings and constrictions of various sizes, both within the individual pores and from one pore to another.

If the pore length and breadth are much greater than the pore widths of interest, the motion of the molecules within these pores will be essentially that observed in the MD simulations of diffusion between infinite graphitic surfaces. MacElroy *et al.*⁹ have shown that this is likely to be so for real CMSs.

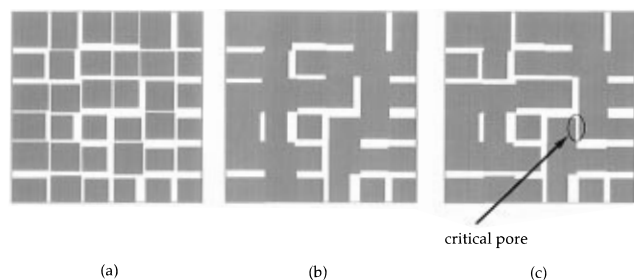


Figure 4. Schematic illustration of the critical path analysis using a two-dimensional pore network.

At first sight, it might be expected that a network composed of pores of many sizes would exhibit a lower selectivity than a single pore. For example, consider a PSD centered around $w = 0.209$ nm. For an individual pore of this size, $R = 20.2$. It might be expected that the presence of pores slightly larger than 0.209 nm would allow the diffusing molecules to bypass pores of this size leading to a smaller value of R . Certainly, this is the case for a system of parallel pores. However, it turns out not to be so for a realistic, interconnected network of the sort found in real CMSs. The critical path analysis (CPA) of Ambegaokar *et al.*¹⁴ explains why.

Ambegaokar *et al.* considered the problem of hopping conduction in semiconductors and showed that, provided the conductance distribution is sufficiently wide, most of the current passes through controlling resistances of a certain critical value. In the language of our problem, the CPA suggests that the kinetic separation in the CMS pore network is dominated by pores of this critical size and that pores much smaller or larger than this value play little role in the separation.

The physical basis of the CPA may be understood by considering the following thought experiment, illustrated using Figure 4 which is a schematic illustration of the two-dimensional analogue of a CMS pore network. (For convenience, the network nodes in this diagram are simply the intersections of the parallel-sided pores; as they are assumed to offer no resistance to diffusion, their actual size in the model is arbitrary.) Consider a pore network defined by a PSD and a mean coordination number, Z , shown in Figure 4a. We remove all of the pores from the network and then replace them, in their original locations, in order of decreasing diffusional conductance (i.e., beginning with the largest pore). We monitor the diffusion process from left to right across the network as we carry out this procedure. As the first few pores are replaced, there is no transport path from one side of the system to the other and the effective diffusivity of the network is zero (Figure 4b). This remains so until a sufficiently large proportion of the pores have been replaced for a percolating cluster of pores to be formed (Figure 4c). For a sufficiently wide PSD, diffusion is now controlled by the last "critical" pore to be replaced, i.e., the one that completed the percolating cluster. All of the pores that were previously replaced are larger than the critical pore and, as they are effectively in series with that pore, they exert little resistance to diffusion and may be neglected. The remainder of the pores are now replaced, restoring the complete network shown in Figure 4a. As all of these pores are smaller than the critical pore, and essentially in parallel with it, they play little part in the diffusion process and hence may be neglected. Thus, the CPA argues that the molecular sieving properties of the original, complete, CMS pore network are essentially those of the

critical pore. This suggests that molecular sieving should be possible even for wide PSDs, provided the critical pore size of a CMS network is in the appropriate range.

In the usual interpretation of the CPA, where it is applied to pure species diffusion or its analogue, the analysis becomes exact for a PSD of infinite width. For the present problem of binary selectivity in a CMS, it is the distribution of the diffusion coefficient ratio, R , rather than the PSD itself that matters. As R approaches the ratio of the bulk diffusion coefficients for large pore widths, the distribution of R is always finite, even for an infinitely wide PSD. Thus, our CPA is approximate, even in that limit.

The critical pore size is calculated using the CPA as follows. The PSD is defined in terms of the probability density function for the pore width, $f(w)$ ($=dN/dw$, where N is the pore number), normalized so that

$$\int_0^\infty f(w) dw = 1 \quad (2)$$

The percolating cluster of pores is formed when the cumulative fraction of the pores that are larger than the critical pore size, w_{crit} , is equal to the percolation threshold of the network, p_c .

$$p_c = \int_{w_{\text{crit}}}^\infty f(w) dw \quad (3)$$

The percolation threshold is the minimal fraction of the pores that must be in place for a sample-spanning cluster to be formed. The value of p_c primarily reflects the connectivity of the network and is relatively insensitive to other aspects of the network topology. All three-dimensional networks follow, to a good approximation, the empirical rule¹⁵

$$Zp_c \approx \frac{3}{2} \quad (4)$$

Combining eqs 3 and 4, we obtain the relationship between w_{crit} and the structural characteristics of the CMS pore network (expressed in terms of Z and $f(w)$).

$$\frac{3}{2Z} = \int_{w_{\text{crit}}}^\infty f(w) dw \quad (5)$$

In summary, the CPA suggests that, for specified values of $f(w)$ and Z , a CMS pore network should exhibit the same value for the diffusion coefficient ratio, R , as a single pore of width, w_{crit} , and that this value can be calculated from eq 5.

Before applying the CPA, we must first assess its accuracy. This requires the generation of accurate numerical solutions for diffusion in a specific model pore network. We have used a network based on the simple cubic lattice.

Our model network is generated by deleting some of the bonds to obtain the desired coordination number ($Z = 6$ for the original simple cubic lattice) and then distributing REG pores along the surviving bonds, choosing the pore widths at random from the imposed PSD. As the network is based on a regular lattice, it misses some of the disorder in a real amorphous solid; for example, the pore length is constant in our model. However, it is known that once the PSD and a value of Z have been set, other aspects of the topology have little influence on the

(14) Ambegaokar, V.; Halperin, B. I.; Langer, J. S. *Phys. Rev. B: Condens. Matter* **1971**, 4, 2612.

(15) Sahimi, M. *Applications of Percolation Theory*; Taylor and Francis: London, 1994.

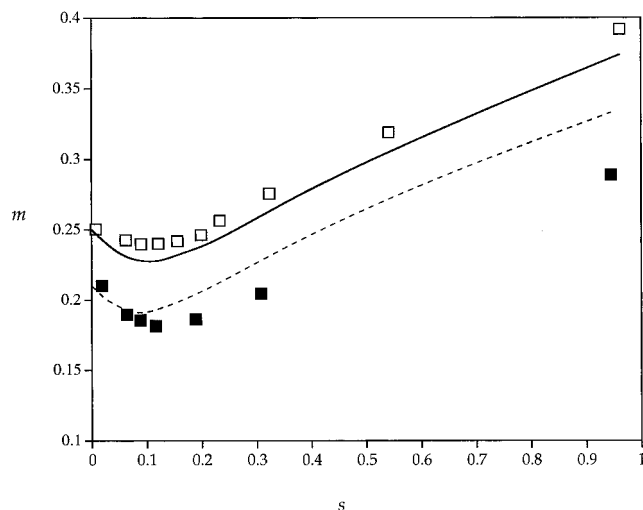


Figure 5. Comparison between CPA (curves) and MC-REMA (symbols) for $w_{\text{crit}} = 0.21$ nm (solid squares/dashed curve) and $w_{\text{crit}} = 0.25$ nm (open squares/continuous curve).

transport properties,^{16,17} so that general conclusions may be drawn from a comparison between the CPA and a solution to diffusion in this model pore network.

We used the Monte Carlo renormalized effective medium approximation (MC-REMA) method of Zhang and Seaton¹⁸ to calculate the diffusion coefficients of oxygen and nitrogen. This method is known to give very accurate diffusion coefficient results for the simple cubic lattice.¹⁸ The application of this method to diffusion in CMSs is described in detail by MacElroy *et al.*⁹ The accuracy of the CPA was assessed by solving eq 5 to generate combinations of the mean and the standard deviation of the PSD to give a specified value of w_{crit} , and then using the MC-REMA method to find combinations of these parameters to give the value of R corresponding to a single pore of that size.

In the CPA and MC-REMA calculations, the PSD was described by the log normal distribution

$$f(w) = \frac{1}{\sqrt{2\pi}\sigma w} \exp\left[-\frac{(\ln w - \mu)^2}{2\sigma^2}\right] \quad (6)$$

where μ and σ are parameters. The mean, m , and the standard deviation, s , of the distribution are given by

$$m = e^{(\mu + 0.5\sigma^2)} \quad (7)$$

$$s + (e^{(2\mu + 2\sigma^2)} - m^2)^{1/2} \quad (8)$$

Figure 5 shows the CPA and MC-REMA results for the two pore networks with $Z = 4.5$ and $w_{\text{crit}} = 0.21$ nm (corresponding to $R = 20$) and $w_{\text{crit}} = 0.25$ nm (corresponding to $R = 2.8$). The CPA curves are the loci of combinations of m and s that give networks with these critical pore widths. Pore networks close to a critical path locus are predicted by the CPA to have values of R close to that of the critical pore width. Networks well above the locus exhibit much lower kinetic selectivity. Networks well below the locus either exhibit higher selectivity or, further away, do not permit diffusion at all.

As might be expected for such a simple theory, the CPA does not quantitatively reproduce the MC-REMA results.

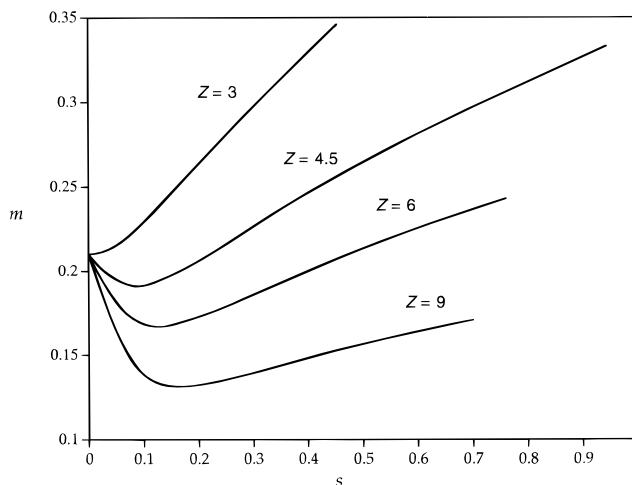


Figure 6. Critical path loci for various values of Z .

However, the shape of the curves is similar, and the quantitative differences are not large, even for narrow PSDs where the CPA is expected to be least accurate. This comparison suggests that the CPA is a physically realistic way to view the separation mechanism and that it provides a useful way to investigate the relationship between pore structure and kinetic selectivity.

Figure 6 shows the critical path loci for $w_{\text{crit}} = 0.21$ and various values of Z . These results may be interpreted physically as follows. As Z increases, a diffusing molecule is offered an increasing number of possible routes to the interior of the CMS and a smaller mean pore size is required (for a given value of s) to ensure that the molecule cannot bypass the constrictions that carry out the kinetic separation. The existence of a minimum for a large Z (and hence a small p_d) arises because for low values of s , $w_{\text{crit}} < m$, while for wider distributions, $w_{\text{crit}} > m$. This behavior is not specific to the log normal distribution but rather is a consequence of the fact that the PSD of a porous solid is physically bounded on one side by $w = 0$ but is unbounded on the other side.

It is of interest to consider the sieving behavior of the network in the limit of high connectivity, $Z \rightarrow \infty$ (and $p_c = 0$), where a diffusing molecule can pass from one pore to any other pore. In this limit, from eq 5, the critical pore size must be essentially the largest pore present in the network. In physical terms, if any pores larger than w_{crit} were present, these would provide channels of high permeability to both species, reducing the sieving effect of the network. In contrast, in the limit of low connectivity ($Z = 1.5$, $p_c = 1$), eq 5 shows that all of the pores must be larger than the critical pore. In physical terms, all transport must pass through the very smallest pores in the network.

4. Summary and Discussion

We have carried out MD simulations for the diffusion of oxygen and nitrogen at the individual pore level. The simulations show that the REG model can give kinetic selectivities in the same range as those observed experimentally for CMSs, over a relatively narrow range of degree of etching. The critical path analysis of diffusion in a model CMS pore network composed of REG pores gives a physical interpretation for the sieving behavior of a network containing a range of pore sizes and quantifies the effect of the pore structure (expressed in terms of the PSD and Z) on the sieving behavior. According to the CPA, pore networks with both narrow and wide PSDs can

(16) Jerauld, G. R.; Scriven, L. E.; Davis, H. T. *J. Phys. C: Solid State Phys.* **1984**, 17, 3429.

(17) Arbabi, S.; Sahimi, M. *Chem. Eng. Sci.* **1991**, 46, 1739.

(18) Zhang, L.; Seaton, N. A. *AIChE J.* **1992**, 38, 1816.

carry out molecular sieving, provided a pore of width w_{crit} (defined by eq 5) can itself act as a sieve.

Other pore structure models are possible and may be closer than our model to the structure of some real CMSs. For example, in our model, the heterogeneity of the pore network is represented at two length scales: at the atomic scale, by the repeated openings and constrictions within a single REG pore, and at the pore scale, by the difference in the diffusion coefficient from pore to pore (with the connectivity of the network also entering on this scale). One could also include structure on the atomic scale at the nodes of the network by including an atomic description of the pore entrance, in which case the interplay between the connectivity and the pore geometry would differ from that of our model. (The mass transfer resistance associated with the pore entrances has been studied by Ford and Glandt.^{19,20})

Clearly, the numerical results presented here are specific to the model pore network that we have chosen. Nevertheless, the CPA result that diffusion (and hence kinetic separation) is controlled by pores close in size to w_{crit} , which is related to the statistical geometry and topology of the pore network by eq 5, is quite general. The assumption underlying the CPA is simply that the pore space of the CMS can be treated as a network of pores, i.e., that it can be separated conceptually into (i) elements that provide resistance to diffusion—pores, or simple constrictions—and (ii) elements at which a diffusing molecule can take one of several alternative paths—nodes—at which conservation of mass is satisfied.

LA9510644

(19) Ford, D. M.; Glandt, E. D. *J. Membr. Sci.* **1995**, 107, 47.

(20) Ford, D. M.; Glandt, E. D. *J. Phys. Chem.* **1995**, 99, 11543.